Available online at www.sciencedirect.com
ScienceDirect
Trans. Nonferrous Met. Soc. China 30(2020) 3078−3092
Transactions of Nonferrous Metals Society of China
www.tnmsc.cn

Effect of zinc powder content on tribological behaviors of brake friction materials

Yang YANG[1,2*], Lu-xin LIANG[1*], Hong WU[1], Bo-wei LIU[1,2], Hui QU[2], Qi-hong FANG[3]

1. State Key Laboratory of Powder Metallurgy, Central South University, Changsha 410083, China;
2. Hunan Boyun Automobile Brake Materials Co., Ltd., Changsha 410205, China;
3. State Key Laboratory of Advanced Design and Manufacturing for Vehicle Body, Hunan University, Changsha 410082, China

Received 8 February 2020; accepted 17 August 2020

Abstract: Brake friction materials with different zinc powder contents (0, 2, 4, 6, 8 wt.%) were fabricated via powder metallurgy method. The results indicate that with the increasing zinc powder content, the density and thermal conductivity of the materials gradually increase, while the hardness decreases monotonously. With increasing zinc powder content, the curve of the nominal friction coefficient shows fluctuating trend but the lowest friction coefficient also shows an increase. However, the wear rate and braking noise of the friction material monotonously decrease with increasing zinc content. This effect may be attributed to the transformation of the tribological mechanism from adhesive wear and abrasive wear to adhesive wear. The brake friction material with 4 wt.% zinc powder exhibits both the best tribological and noise performance.

Key words: zinc powder content; brake friction material; tribological behavior; braking noise

1 Introduction

With the rapid development of the automobile industry, the market demand for automotive brake friction materials is growing substantially. Currently, automobile brakes are mostly fabricated using asbestos-free resin-based friction materials [1], including the semi-metallic, low-metallic, and hybrid fiber-reinforced friction materials [2−4]. Among them, semi-metallic and low-metallic materials are well accepted as brake friction materials, while steel fibers are the most commonly used metal reinforcing fibers [5−8]. However, steel fibers are prone to rust, which reduces their strength and increases the wear rate of the friction materials [9,10]. The corrosion products from steel fibers also create substantial damage to the brake disc, especially when the steel fiber content is excessively high. Further, the rust products can easily cause harsh noises and tremors during braking, which will seriously affect the safety and comfort of driving [9,11,12]. Thus, it is urgent to develop high-performance automotive brake semi-metallic friction materials possessing eco-friendly, durable and very stable properties.

When the kinetic energy absorbed by a brake pad is increased during braking due to increased load, speed and/or braking time the temperatures of both the friction material and rotor increase [13]. BAKLOUTI et al [14] reported that polymeric materials could melt and the resins binding the

Foundation item: Project (2016YFB1100103) supported by the National Key Research and Development Program of China; Project (KC1703004) supported by the Science and Technology Planning Project of Changsha City, China; Project (2018ZZTS127) supported by the Fundamental Research Funds for the Central Universities of Central South University, China

Corresponding author: Hong WU; E-mail: wuhong927@126.com
*Yang YANG and Lu-xin LIANG contributed equally to this work.

DOI: 10.1016/S1003-6326(20)65444-9

friction material could vaporize during braking, which prevents the friction material from contacting the rotor, and, hence, reduces the coefficient of friction. As the surface temperature increases, the friction coefficient gradually decreases, and hence, the braking efficiency decreases. STOICA et al [15] suggested that the amplitude of the stick-slip process increases with increasing contact pressure and sliding speed, which leads to an in audible noise. Zinc is more chemically reactive than iron and can electrochemically react with iron in an oxygen-containing aqueous atmosphere. Normally, a thin, dense zinc oxide film will form on the surface of zinc powder at room temperature, which, to a certain extent, can inhibit the corrosion of friction materials. Being environmentally friendly, ZnO particles have been used for various applications in tribology [16]. Zinc powder has a low melting point and a lot of advantages, such as good ductility and good thermal conductivity [17]. Further, it is non-toxic and is frequently added to biomaterials to improve the biological properties [18−20]. Zinc powder can not only inhibit corrosion but also stabilize the friction coefficient and reduce the wear of friction materials [21]. KALYANI et al [17] suggested that zinc oxide was doped with magnesium, promoting the formation of slip systems and lower shear strength of $Zn_{0.88}Mg_{0.12}O$. Therefore, zinc powder is used as an additive to improve the tribological properties of brake friction materials [22,23]. Nevertheless, the mechanisms whereby zinc powder improves brake friction materials, especially the role of zinc powders in high-temperature friction remain controversial.

In this work, the effects of zinc powder content on the physical properties, mechanical properties, tribological properties and braking noise of brake friction materials were systematically investigated, and the related mechanisms were discussed.

2 Experimental

2.1 Materials

Modifications were made to an existing mature low-metal formula friction material provided by Changsha Hualiu Metallurgical Powder Co., Ltd., by adding 0, 2, 4, 6 and 8 wt.% zinc powder (99.9% purity), simultaneously, reducing the barium sulfate (98.5% purity) content, see Table 1. The chemically-stable barium sulfate is a heavy filler, whose low volume fraction means that it has little impact on the wear and noise performance of friction materials. Therefore, the change in the zinc powder content can be considered as the main factor affecting the physical properties, mechanical properties and braking properties of the specimens.

2.2 Fabrication

A simple homebuilt high-speed mixer was employed to blend the materials listed in Table 1. The mixing time was 3 min, and the rotation speed of the mixer was 1400 r/min. A Passat rear brake pad (D1348) was selected as the specimen and molded by a one-step molding method on a Wanda JFY60-type air pressure machine. Each cavity was filled with 120 g of the blend, and then heat-cured in a compression-molding machine under a pressure of 11.5 MPa at (160±5) °C for 7−8 min. The pads were post-cured in a furnace (KSL−1200X, Hefei, China) at 150 °C for 8 h, and then the surfaces of the pads were polished with a flat-grinding machine to produce the desired thickness and surface finish. The roughness of the tested brake friction materials is in the range of 6.3−12.5 μm. Photographs of brake friction material are shown in Fig. 1.

2.3 Phase composition and physical properties

The pad was cut into specimens with a diameter of 10 mm and a thickness of 3 mm for

Table 1 Basic friction material compositions (wt.%)

Specimen No.	Phenolic resin	Nitrile rubber	Zinc	Aramid pulp	Graphite	$BaSO_4$	Others
Z1	6	3	0	1	8	15	67
Z2	6	3	2	1	8	13	67
Z3	6	3	4	1	8	11	67
Z4	6	3	6	1	8	9	67
Z5	6	3	8	1	8	7	67

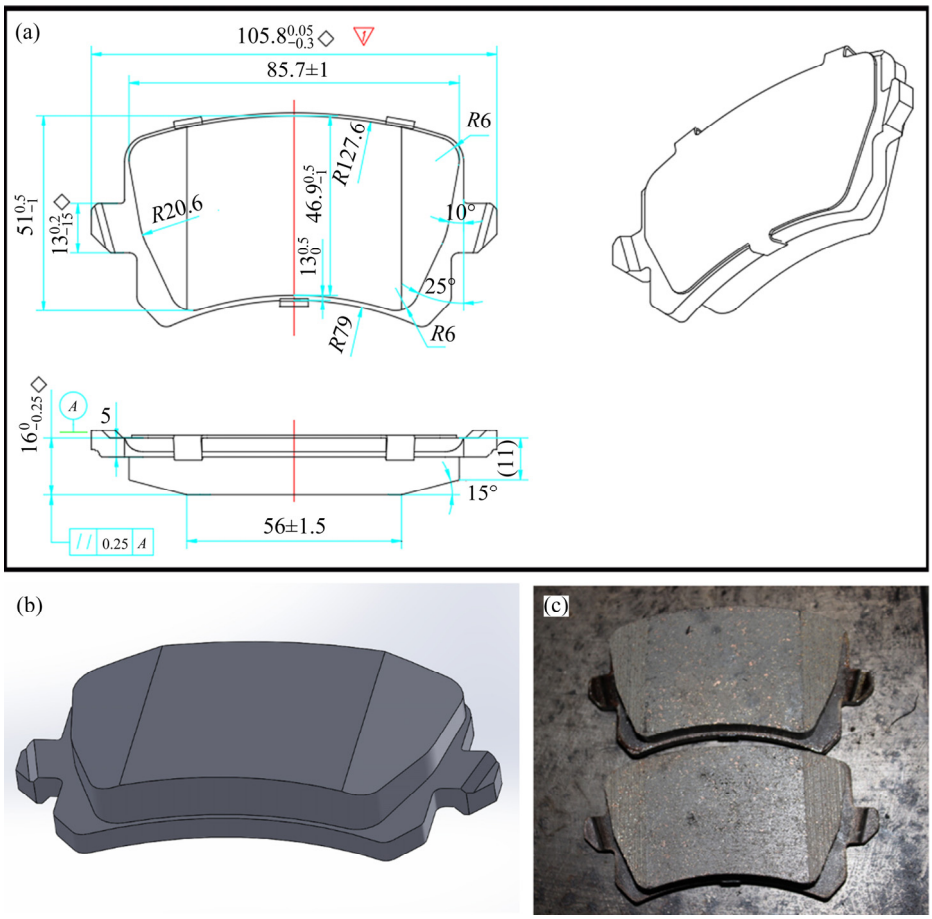

Fig. 1 Computer-aided design graphics (a), 3D image (b) and photograph (c) of brake friction material (Unit: mm)

measuring the phase compositions and physical properties. The worn surfaces of the specimens were characterized using a scanning electron microscope (SEM, JSM−6490LV) operated at 20 kV, and the elemental composition of the worn surface was analyzed using energy dispersive spectroscopy (EDS). The phases present in the debris were determined by using an X-ray diffractometer (XRD, Rigaku D/Max 2500) employing Cu K_α radiation at a scan rate of 5 (°)/min and an accelerating voltage of 25 kV.

The density of each specimen was determined by using the method of Archimedes principle according to the JC/T 685—1998 friction material density test method. The pH values of the friction materials were measured using a pH meter according to JASO C458—1986, which is the standard test procedure for the pH of brake linings, gaskets and clutch friction plates of automobiles. The apparent porosity of the specimen was examined by the method of oil immersion according to the QC/T 583—1999 test method for the apparent porosity of automobile brake linings. The thermal conductivity of each friction material was evaluated by the method of thermal pulse according to the Chinese National Standard GB11108—89. The thermal conductivity tests were performed on a JR−3 laser thermal conductivity instrument manufactured by the Changsha Zhongda Precision Instrument Co., Ltd., China.

2.4 Mechanical properties

The hardness of the specimens was determined using an HR−150A Rockwell hardness tester with a load of 980 N equipped with a steel ball indenter with a diameter of 12.7 mm. The compressibility tests were conducted on a model 1620 compression machine manufactured by the Link Engineering Company under the rule of the ISO 6310 road vehicle brake lining compression strain test. The area of the compression piston was 11.34 cm^2, and a pressure of 16 MPa was adopted to test the specimens within 2 s. This test was repeated three times. The shear strength testing was performed on a universal hydraulic testing machine, with a loading rate of (4.5±1.0) kN/s.

2.5 Friction and wear measurement

The friction and wear performances were tested in accordance with the protocol listed in SAE J2522 on a LINK 3000 inertial bench testing machine. The friction performances of different friction materials under different braking speeds, pressures and temperatures were tested in compliance with the SAE J2522 test procedure. The friction material brake noise tests were performed on a LINK 3900 NVH (noise, vibration and harshness) inertia bench testing machine in accordance with the protocol of the SAE J2521 test. The schematic diagrams of LINK 3000 inertial bench testing machine and the LINK 3900 NVH inertia bench testing machine are shown in Fig. 2 and Fig. 3, respectively. The related braking parameters of SAE J2521 noise evaluation test procedure are shown in Table 2 [24].

2.6 Statistical analysis

The pH value, porosity, density and thermal conductivity tests were repeated at least three times for each material. The hardness, compressive strain and shear strength tests were repeated at least 5 times for each material and the data were expressed as mean ± standard deviation.

3 Results

3.1 Powder characterization

As shown in Figs. 4(a) and (b), the zinc powder particles were spherical with particle diameters of 1−5 μm, and the barium sulfate particles were irregularly granular with particle sizes less than 47 μm. The XRD patterns of the zinc powder and barium sulfate are shown in Figs. 4(c) and (d), respectively. The results indicated that all the diffraction peaks in the patterns correspond to zinc and barium sulfate.

3.2 Physical properties

Table 3 lists the physical properties of brake friction materials with five different zinc powder contents. The pH value and porosity exhibited no

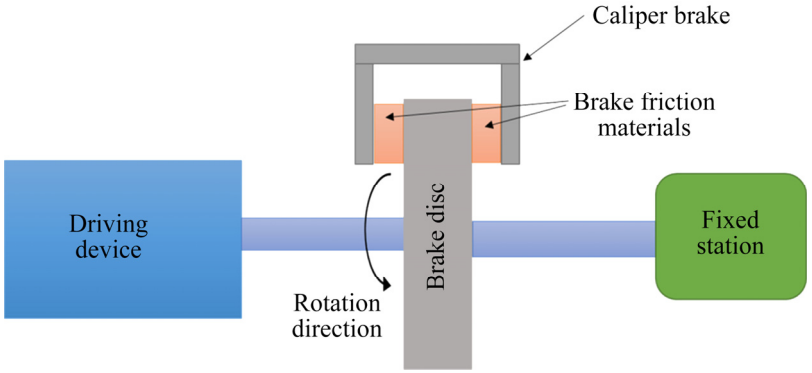

Fig. 2 Schematic diagram of LINK 3000 inertial bench testing machine

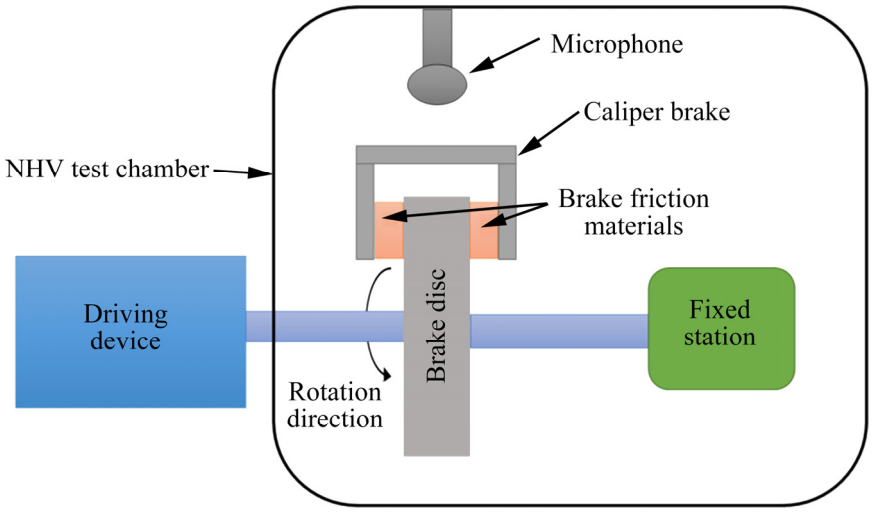

Fig. 3 Schematic diagram of LINK 3900 NVH inertia bench testing machine

Table 2 Related braking parameters of SAE J2521 noise evaluation test procedure [24]

No.	Braking times	Initial braking speed/(km·h^{-1})	Ending braking speed/(km·h^{-1})	Braking pressure/MPa	Initial braking temperature/°C
1	30	80	30	3	100
2	32	80	30	1.5, 3, 1.5, 1.8, 2.2, 3.8, 1.5, 2.6, 1.8, 3.4, 1.5, 2.6, 1.5, 2.2, 3, 4.6, 2.6, 5.1, 2.2, 1.8, 4.2, 1.5, 1.8, 4.6, 2.6, 1.5, 3.4,2.2, 1.8, 3, 1.8, 3.8	100
3	6	80	30	3	100
4	266	3 and 10 alternation	Constant speed	0, 3, 0.5, 2.5, 1,2, 1.5	50−300−50
5	24	50	0	3, 0.5, 2.5, 1,2, 1.5	100, 150 (12 times each)
6	50	−3 and 3 alternation	Constant speed	0, 2, 0.5, 1.5, 1	150, 125, 100, 75, 50 (10 times each)
7	108	50	0	3, 0.5, 2.5, 1, 2, 1.5	50, 100, 150, 200, 250, 200, 150, 100, 50 (12 times each)
8−18	Repeat 3→Repeat 4→Repeat 5→Repeat 6→Repeat 7→ Repeat 3→Repeat 4→Repeat 5→Repeat 6→Repeat 7→Repeat 3				

Table 3 Physical properties of specimens with different zinc powder contents

Specimen No.	Zn content/wt.%	pH	Porosity/%	Density/(g·cm^{-3})	Thermal conductivity/(W·m^{-1}·K^{-1})
Z1	0	10.08±0.05	11.07±0.02	2.82±0.02	9.85±0.06
Z2	2	9.80±0.08	11.01±0.03	2.87±0.03	12.32±0.09
Z3	4	10.05±0.04	11.07±0.02	2.87±0.02	13.26±0.04
Z4	6	9.98±0.02	10.16±0.04	2.92±0.04	15.41±0.12
Z5	8	10.07±0.03	10.79±0.03	2.93±0.03	16.47±0.08

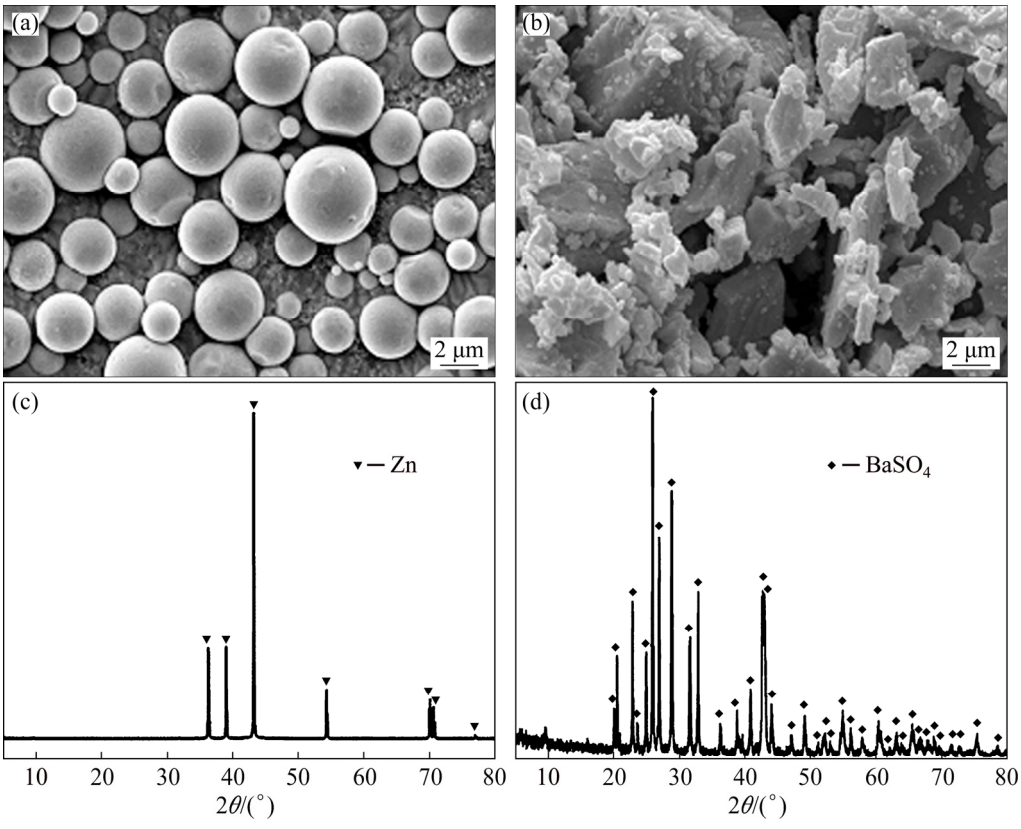

Fig. 4 Secondary electron images (a, b) and XRD patterns (c, d) of zinc powders (a, c) and barium sulfate (b, d)

obvious changes with changes in the zinc powder content. Since the density of zinc powder (7.14 g/cm^3) is higher than that of barium sulfate (4.5 g/cm^3), the density of the friction material slightly increased with increasing zinc powder content. With the increase of the zinc powder content and corresponding decrease of the barium sulfate content, the thermal conductivity gradually increased because the thermal conductivity of zinc powder is higher than that of barium sulfate.

3.3 Mechanical properties

The influences of the zinc powder content on the hardness, compressive deformation and shear strength of friction materials are listed in Table 4. As the zinc powder content increased, the hardness decreased monotonically. By comparison, the compressive strain initially deceased and then increased, while the shear strength of the specimens initially increased and then showed a small decrease with increasing zinc content. Note that the change in hardness amongst the five specimens was <10%. Mohs hardnesses of the zinc powder and the barium sulfate are 2.5 and 3−3.5, respectively. Although the Mohs hardness of barium sulfate is slightly higher than that of zinc powder, the volume fractions of the two materials in the formulation system were relatively low. Hence, there was no considerable difference for compressive strain of the five specimens. The shear strength of the friction materials is attributed mainly to the compatibility of the organic binder, skeleton fiber and various fillers with the phenolic resin. Both zinc powder and barium sulfate are powder fillers with good compatibility with the resin, and these materials will not easily react with other substances at room temperature. Hence, the shear strengths of the specimens are basically at the same level.

Table 4 Mechanical properties of specimens with different zinc powder contents

Specimen No.	Zinc content/ wt.%	Hardness (HRS)	Compressive deformation/μm	Shear strength/ MPa
Z1	0	69.91±0.92	69.51±1.12	4.78±0.95
Z2	2	67.23±0.87	66.63±1.43	4.68±0.67
Z3	4	66.75±0.56	61.55±1.40	5.85±0.48
Z4	6	64.78±0.02	67.85±0.67	5.02±0.34
Z5	8	64.29±0.87	66.83±0.43	5.28±0.54

3.4 Friction properties

The representative nominal friction coefficient (μ_{nom}) which represents the overall friction coefficient level of the material and the lowest friction coefficient (μ_{min}) which represents the ability of the material to resist thermal decay [25] were examined. As shown in Fig. 5, as the zinc powder content increased, the μ_{nom} of the specimen initially increased, then decreased, and finally increased, whereas μ_{min} increased monotonically. These results indicated that the overall friction coefficient of the friction material initially increased first, then decreased, and finally increased with an increase in the zinc powder content, while the ability to resist thermal decay was always enhanced. KUMAR and BIJWE [26] reported that the thermal conductivity of a non-asbestos organic composite was enhanced from 1.55 to 2.41 W/(m·K) by the addition of a metal filler (brass, copper or iron), and that the friction and wear performances of brake materials were improved correspondingly. This result is similar to our study.

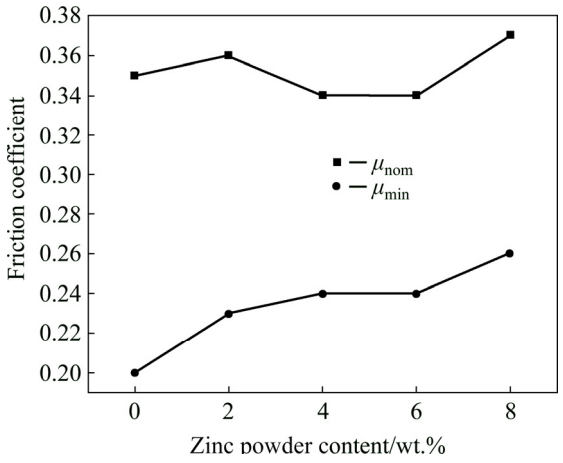

Fig. 5 Nominal friction coefficient (μ_{nom}) and minimum friction coefficient (μ_{min}) as function of zinc powder content of friction materials

To further study the influence of the zinc powder content on the stability of the friction coefficient of the materials, friction coefficient measurements of braking pressure at initial braking speeds of 40, 80 and 120 km/h were performed. As shown in Figs. 6(a−c), as the braking pressure increased, the friction coefficient of the specimen decreased. When the friction test was performed at an initial braking speed of 40 km/h, the friction coefficient of the brake friction material without

zinc powder was the most stable. However, at 80 and 120 km/h, the friction coefficient of the specimen with 4 wt.% zinc powder content was the most stable. This could be attributable to the rapidly rising temperature generated during braking at the initial braking speeds of 80 and 120 km/h (Figs. 6(a−c)). As shown in Fig. 7, the temperatures of the disc were measured by putting a thermocouple in the middle of the friction track on the outer surface of the brake disc. The temperature of brake disc increased with the increase of the initial braking speed, and decreased with the increase of zinc powder content in friction material. As the braking pressure increased, the temperature of the disc gradually decreased. In this study, the speed after braking was only reduced to 40 km/h. Hence, as the braking pressure increased, the braking time decreased and the temperature of the disc decreased.

The variations of friction coefficient with zinc powder content during the first and second high-temperature fades were also examined. As shown in Figs. 6(d) and (e), all specimens exhibited obvious signs of deterioration. However, these results also indicated that the specimen with 4 wt.% zinc powder content exhibited the smallest amount

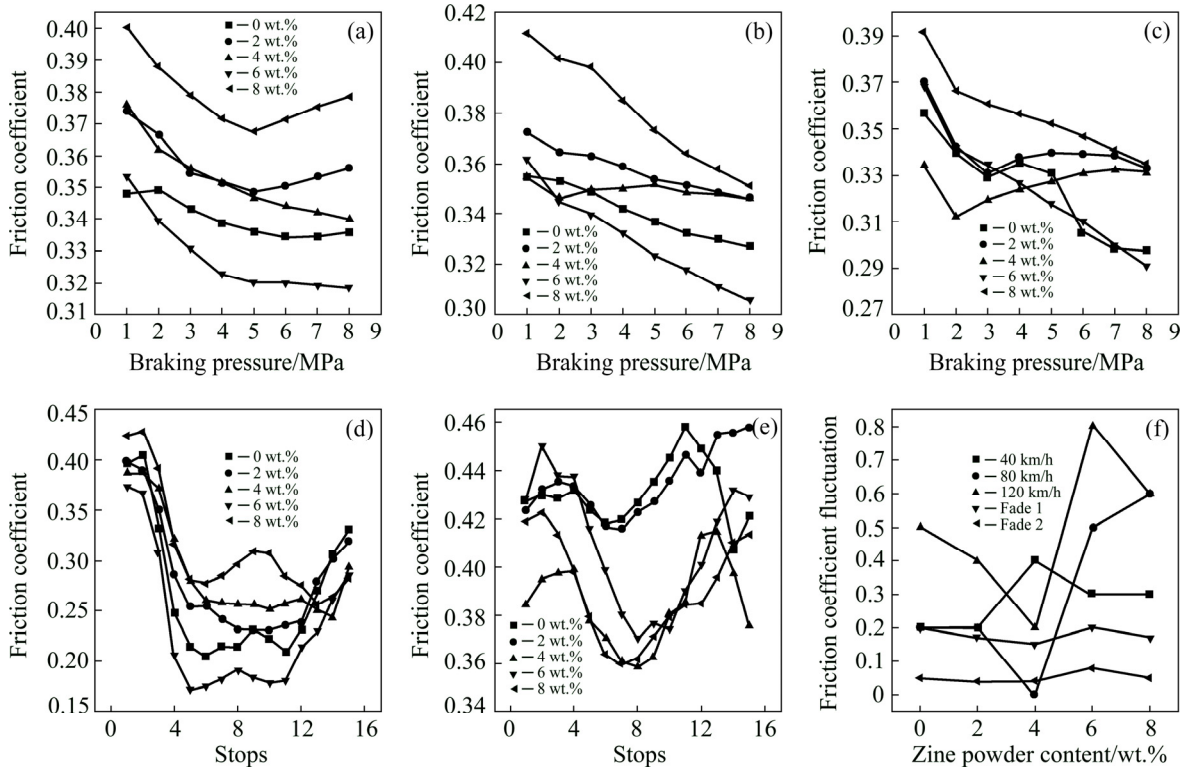

Fig. 6 Effect of zinc powder content on friction coefficient stability of friction materials: (a) 40 km/h braking; (b) 80 km/h braking; (c) 120 km/h braking; (d) Fade 1; (e) Fade 2; (f) Friction coefficient fluctuation

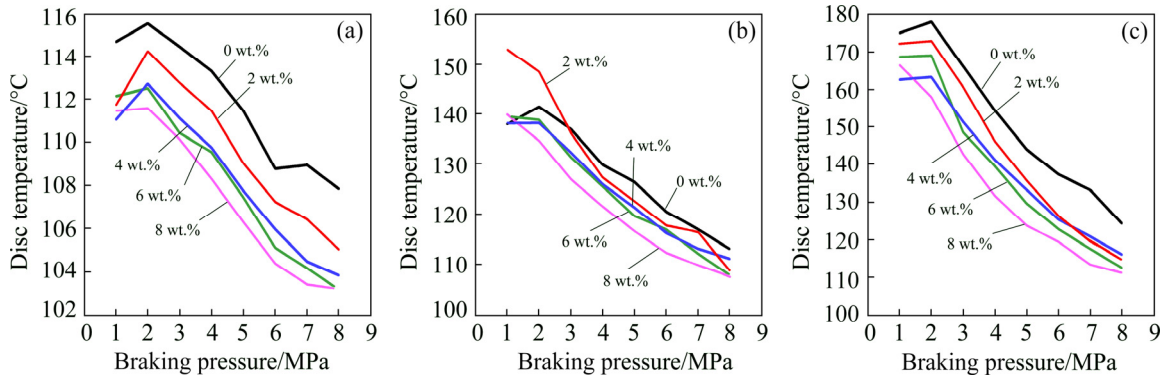

Fig. 7 Disc temperature of friction materials with different zinc powder contents under different braking pressures and speeds at end of each braking period: (a) 40−0 km/h; (b) 80−40 km/h; (c) 120−80 km/h

of deterioration. This result may be due to the formation of friction film which played a very good role in stabilizing the friction coefficient of the interface, resulting in the smallest deterioration rate for this specimen [27]. As shown in Fig. 6(f), the friction coefficients of specimens with different zinc powder contents under different braking conditions were tested. The friction coefficient under various braking conditions slightly decreased or remained unchanged as the zinc powder content increased from 0 to 2 wt.%. The material containing 4 wt.% zinc showed the best high-temperature friction performance except for the case at 40 km/h.

To further verify the influence of the zinc powder content on the friction properties of brake friction materials, the surfaces of the specimens after the friction tests were analyzed using SEM (Fig. 8) and EDS (Fig. 9), and the abrasive dusts from the specimen generated after the friction tests were analyzed using XRD (Fig. 10).

As shown in Fig. 8(a), the surface of the specimen without zinc powders was loose and porous. Only a small amount of friction film was formed, but a large number of irregular particles occurred on the surface, indicating that the wear mechanism of the specimen was mainly abrasive wear [28]. When the zinc powder content increased to 2 wt.%, the zinc powder served as a second binder due to its good ductility and low melting point (Fig. 8(b)), which made the specimen less friable. When the zinc powder content increased to 4 wt.%, the friction film was further completed (Fig. 8(c)). The wear mechanism of this sample was mainly adhesive wear. Zinc powder appeared to be in excess at 6 wt.% Zn, leading to the formation of high hardness, abrasive zinc oxide particles (Fig. 8(d)). At 8 wt.% Zn, large numbers of fragments, oxide films and cracks were formed on the surface of the friction material (Fig. 8(e)). Moreover, in Fig. 8(e), grooves were present on the surface, indicating that the abrasion furrow resistance increased sharply.

As shown in Fig. 9, relatively fine furrows and particles on the surface of the friction material were present for the material containing 8 wt.% Zn. The surfaces of the specimen were relatively complex, and mainly composed of inorganic elements and metallic elements. In addition, large amounts of zinc and oxygen were present in the X-ray spectrum. Secondary electron images and XRD patterns from the wear debris are shown in Figs. 10(a, b) and Figs. 10(c, d), respectively. The wear debris of Specimens Z3 and Z5 showed irregular particles. The XRD patterns showed that zinc oxide peaks are present for debris from Specimen Z5, but not for the debris from Specimen Z3. This indicates that the excess zinc was oxidized on the surface of the friction material Specimen Z5. However, the oxidized zinc content was too low to be found for Specimen Z3.

3.5 Wear behaviors

To analyze the influence of the zinc powder content on the wear resistance of friction materials, the average thickness loss, which reveals the wear rate of the specimens, was measured before and after the SAE J2522 tests. As shown in Fig. 11, the wear thickness of the specimen without zinc powder was 0.24 mm. For an increase in zinc powder content to 2 wt.%, the wear thickness of the specimen decreased rapidly to 0.20 mm. As the zinc powder content further increased to 6 wt.% or 8 wt.%, the wear amount of the specimen continued to decrease.

3.6 Braking noise

The occurrence probability, frequency and decibel value of the braking noise of the friction materials were investigated under different test conditions, such as braking speeds, braking temperatures, braking pressures, and braking directions (Table 2). As shown in Table 2, 1430 times of braking were completed following the protocol of SAE J2521. The noise occurrence probability was obtained by the ratio of number of noises during braking and the total number of times. The noise index was calculated by SAE J2521 program based on the noise occurrence probability, frequency and decibel value of noise. Generally, the higher the noise index is, the lower the noise. As shown in Figs. 12 and 13, the braking noise frequencies for friction materials with different zinc powder contents were distributed mainly in the vicinity of 2, 4, 8 and 16 kHz, and the decibel value was as high as approximately 95 dB. As the zinc powder content increased, the probability of

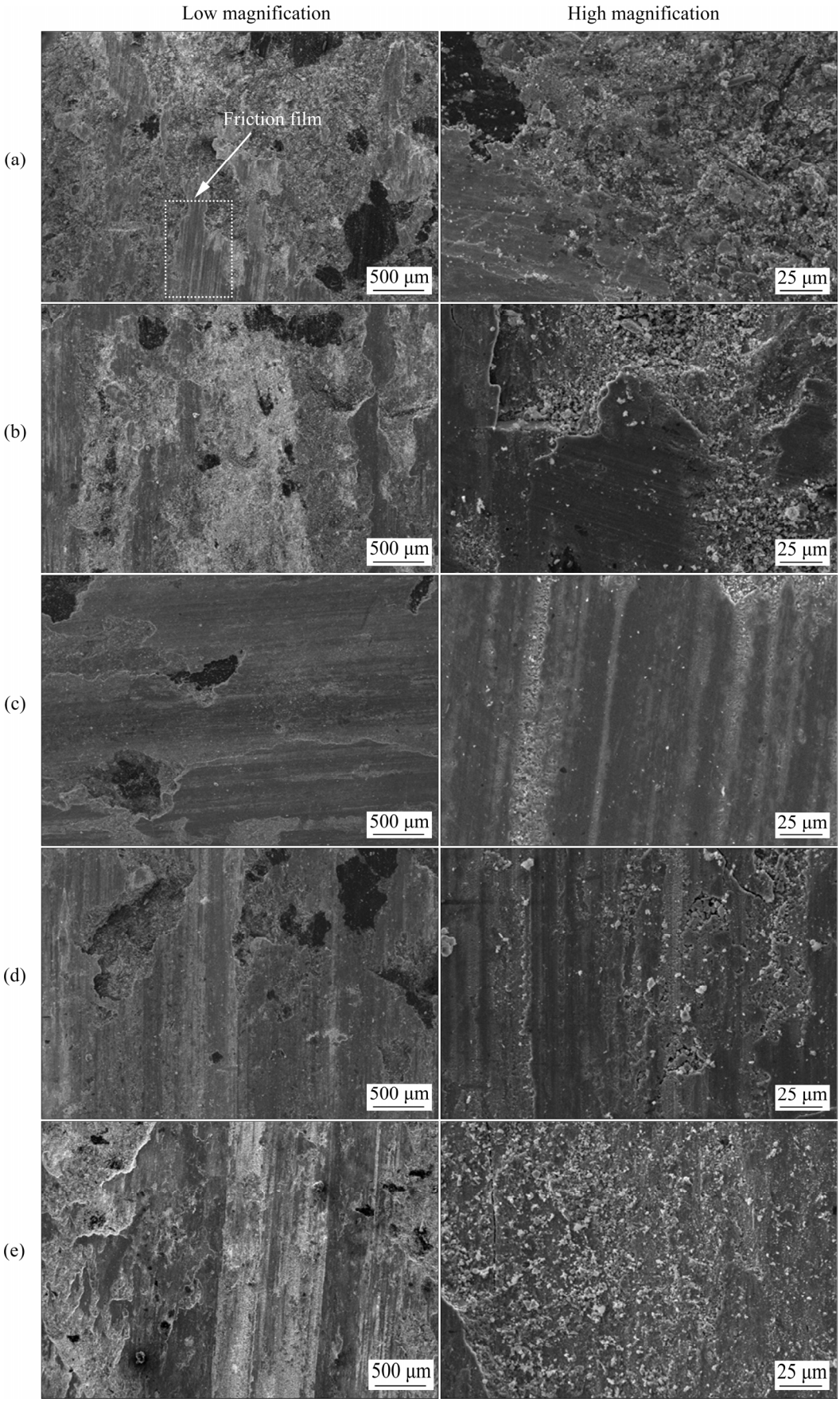

Fig. 8 SEM images of worn surfaces of friction materials with different zinc powder contents: (a) 0 wt.%; (b) 2 wt.%; (c) 4 wt.%; (d) 6 wt.%; (e) 8 wt.%

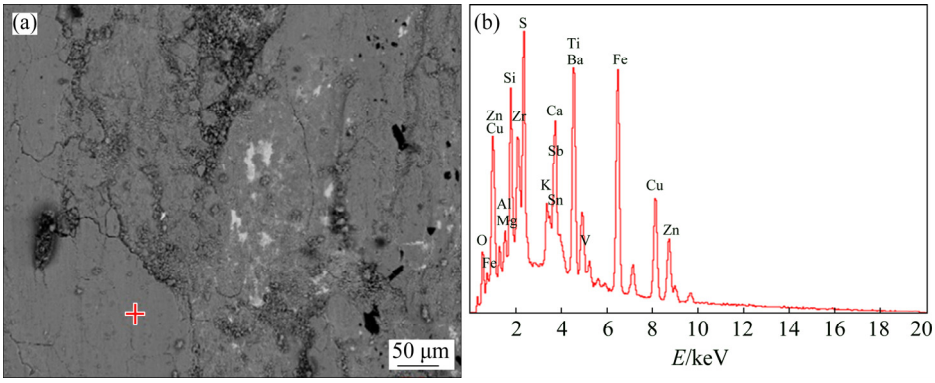

Fig. 9 SEM image (a) and energy dispersive spectroscopy results (b) of friction material surface with 8 wt.% Zn after wear testing

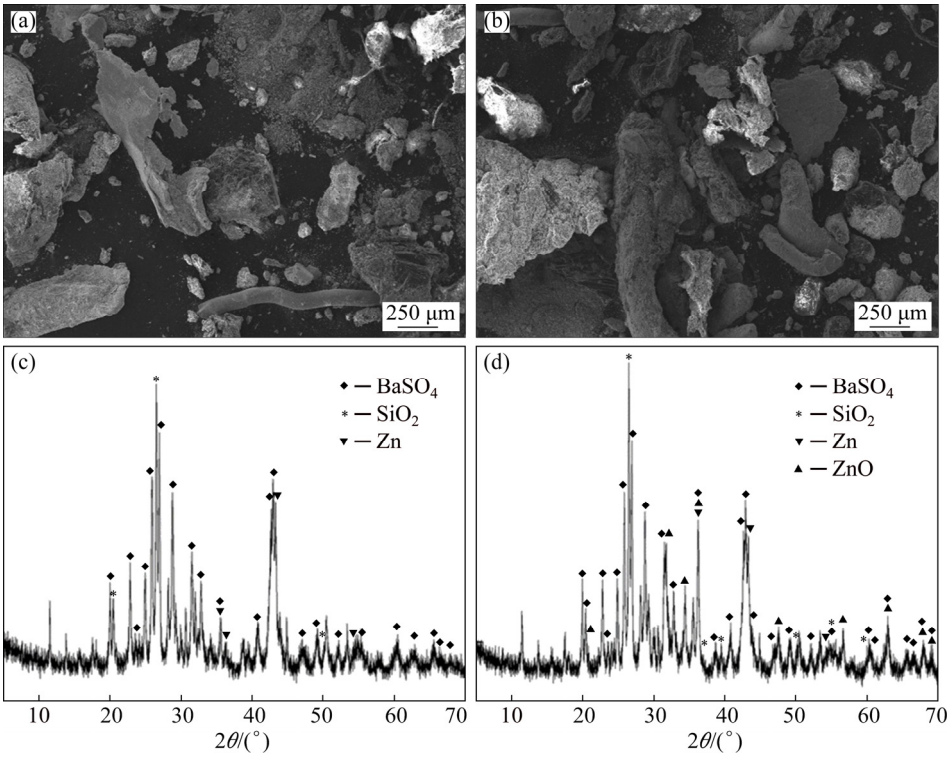

Fig. 10 SEM images (a, b) and XRD patterns (c, d) of debris generated after sliding of Specimens Z3 (a, c) and Z5 (b, d)

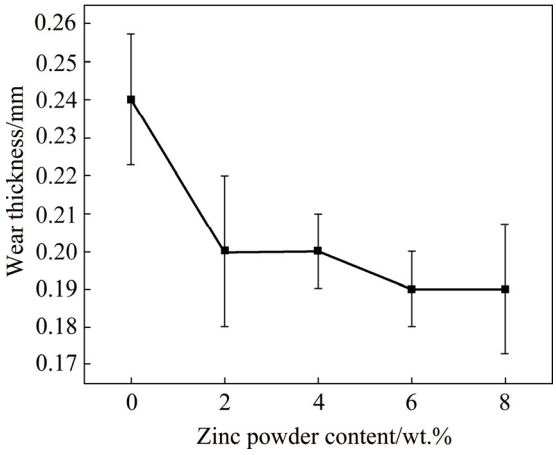

Fig. 11 Wear thickness as function of zinc powder content of friction materials after SAE J2522 test

the noise fluctuated, but the frequency basically remained constant, which was determined mainly by the formulation system and the brake structure. The noise index of the specimen with 4 wt.% zinc powder was significantly lower than that of the specimens with 0 and 8 wt.% zinc powder. As the zinc powder content increased, the braking noise probability in the brake friction materials first decreased and then increased, whereas the comprehensive noise index first increased and then decreased (Fig. 13). The braking noise probability (1.4%) of specimen with 4 wt.% zinc powder was the lowest among the tested specimens, while the comprehensive noise index (8.8) was the highest.

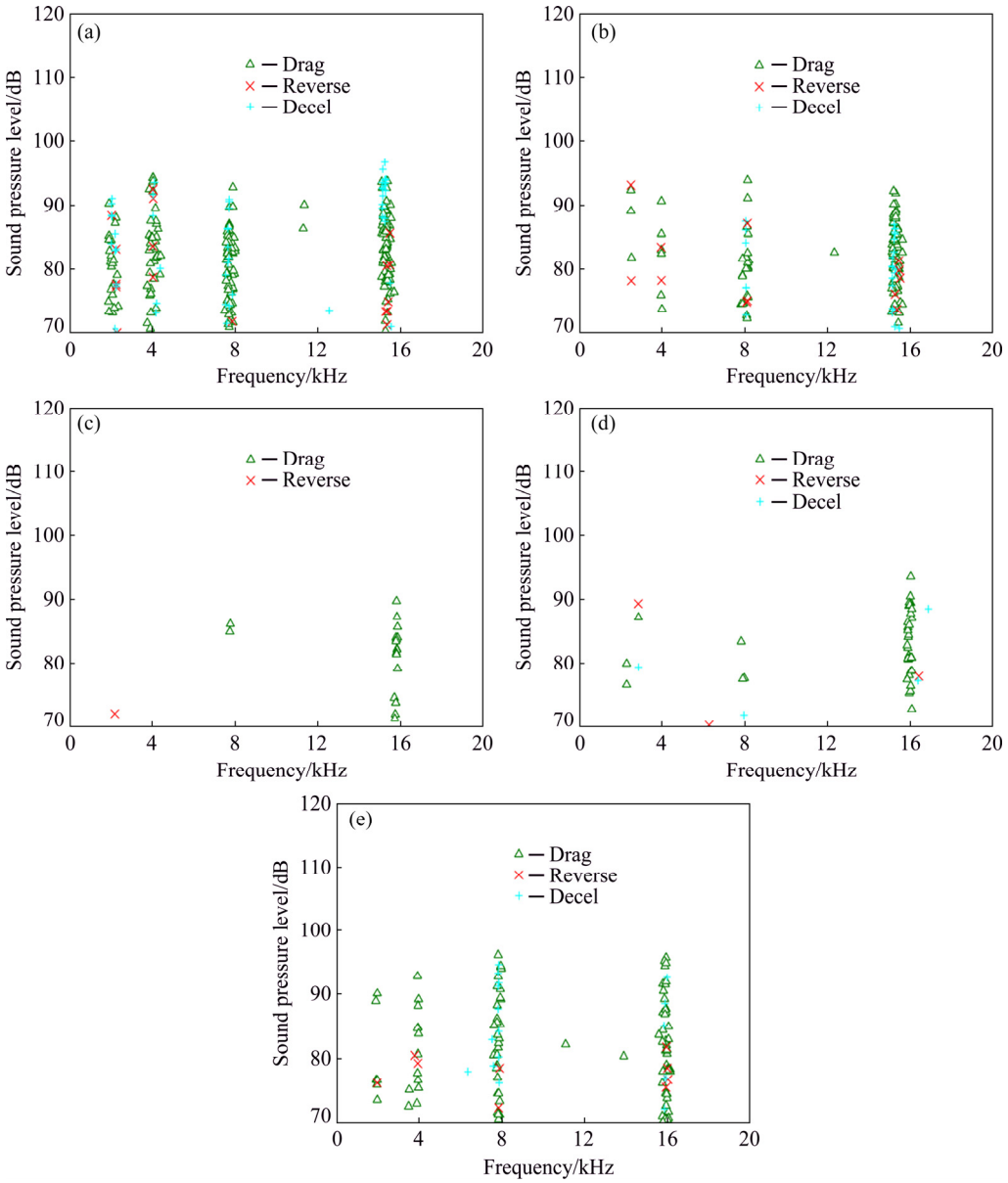

Fig. 12 Braking noise occurrence of specimens with different zinc powder contents: (a) 0 wt.%; (b) 2 wt.%; (c) 4 wt.%; (d) 6 wt.%; (e) 8 wt.% (The braking sound with value above 70 dB is recorded as braking noise. The Drag, Reverse and Decel represent three modes of noise testing)

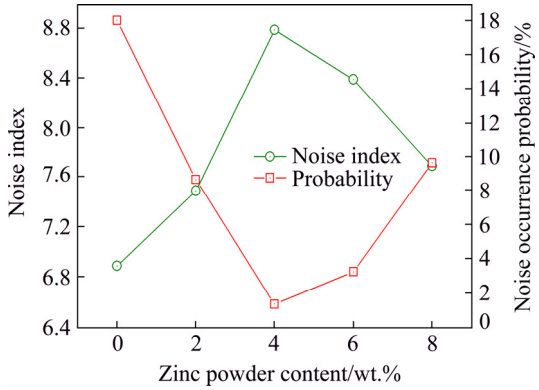

Fig. 13 Index and occurrence probability of braking noise for specimens with different zinc powder contents

4 Discussion

4.1 Friction and wear behaviors

In this study, the μ_{nom} of the specimen increased first, then decreased, and finally increased, whereas μ_{min} continuously increased with the increase of zinc powder. This behavior may be attributed to the transition of wear mechanism due to the addition of zinc powder. According to adhesive wear model (Archard equation) [29]:

$$K=VH/(WL) \quad (1)$$

where K is the friction coefficient, V is the wear

volume of the contact surface, H is the Brinell hardness, W is the normal load, and L is the sliding distance. From Eq. (1), the friction coefficient of a material is proportional to hardness and wear volume, and inversely proportional to sliding distance and normal load. The hardness of specimens shows decreasing trend (Table 4) with increasing zinc powder content. Therefore, the friction coefficient of specimens shows a decreasing trend according to Eq. (1). However, the nominal friction coefficient of specimens showed a fluctuating trend, i.e. Specimens Z3 (4 wt.%) and Z4 (6 wt.%) showed lower nominal friction coefficient than other specimens (Fig. 5).

For the zinc-free material (Z1), a large number of irregular particles are present on the worn surface (Fig. 8(a)), indicating abrasive wear [28,30]. The phenolic resin and rubber will largely decompose when the temperature exceeds 300 °C, leading to bonding failure. As the surface oxide film was continuously destroyed, the actual friction contact area was reduced [31]. Thus, the friction coefficient of this specimen was low but the wear volume of this specimen was high. When 2 wt.% zinc powders were added into brake friction materials (Fig. 8(b)), the bonding strength between the matrix and overlying oxide film was strong. The zinc powder was likely softened during the wear testing due to the rise in temperature, resulting in the increase of the friction coefficient. The wear mechanisms appeared to consist of both adhesion wear and abrasive wear. GAO et al [32] suggested that the softened zinc powder could produce adhesion, which formed a strong mutual adhesion between the zinc powder and the material fiber, resulting in an increase of the friction coefficient. Hence, Specimen Z2 exhibited a higher friction coefficient and a lower wear volume than Specimen Z1. When the zinc powder content increased to 4 wt.% (Specimen Z3) and 6 wt.% (Specimen Z4), the oxide film covered the surface more fully, and high hardness, abrasive zinc oxide particles were formed (see Figs. 8(c) and (d)). These induced the transition of the wear mechanism from a combination of adhesive wear and abrasive wear to solely adhesive wear, giving rise to the decrease of the friction coefficient and wear thickness [33,34]. BAI et al [35,36] suggested that the transition of wear mechanism from adhesive to abrasive led to the increase of wear rate for diamond-like carbon films. In addition, the oxide film could be considered as a lubricant on the surface of friction materials. ZHAI and ZHOU [37] reported that solid superlubricity from the nanoparticle significantly reduced the properties of materials' stiction, friction and wear. Hence, the wear mechanism and solid superlubricity of the surface have an important effect on the friction and wear performance. In a previous study, the zinc oxide was doped with magnesium, promoting the formation of slip systems, which led to a lower shear strength and improved the wear resistance [17]. When the zinc powder content increased to 8 wt.%, a large number of fragments, oxide films and cracks were formed on the surface of Specimen Z5 (Figs. 9 and 10). Part of zinc powders on the surface of Specimen Z5 were oxidized at the high temperature, and then spalled off to form abrasive particles with a relatively high hardness (Mohs hardness of 5.5) [38], which caused the transition of the wear mechanism from adhesive wear to abrasive grooves and adhesive wear. The friction and wear of the film increased due to the adhesion and plowing at a large load. The number of grooves caused by the abrasive particles obviously increased. Therefore, the friction coefficient and wear volume of Specimen Z5 further increased.

The lowest friction coefficient showed an increasing trend with an increase of the zinc powder (Fig. 5), when the temperature of the brake disc exceeded 250 °C after the second braking. At this temperature, the organic adhesives, such as phenolic resin and rubber, in the brake friction material would have decomposed, resulting in the bond failure [23]. However, the zinc powder gradually improved the thermal conductivity of the brake friction materials, which resisted the decomposition of this organic binder [38]. Thus, the thermal degradation of the brake friction material was reduced. The zinc powders were substantially oxidized during the friction process at high test temperature, and the resulting zinc oxide formed abrasive particles on the friction surface. The wear resistance of brake friction materials was improved due to abrasive particles, resulting in the increase of minimum friction coefficient (see Fig. 5).

4.2 Braking noise behavior

The generation of noise is related to vibration, while the generation of vibration is related to the

surface state of the brake friction material [39]. Different surface states of brake friction material could produce differences in vibration and noise [40]. As the zinc powder content increased from 0 to 4 wt.% (Fig. 8), there were fewer irregular furrows and pits on the friction surface. The oxide film coverage of the brake friction material became complete with increasing zinc content, which continuously reduced the changes of the real friction contact area. Therefore, the braking noise of the friction materials decreased with increasing of zinc powder content from 0 to 4 wt.%. However, the numbers of zinc oxide abrasive particles and debris formed on the wear surface increased due to the oxidation and rupture of the surface when the zinc powder content exceeded 6 wt.% (Fig. 10). Abrasive debris fell off from the friction pair and adhered to the brake disc, resulting in the change of the disc thickness. More importantly, the change of the brake disc thickness would force the piston of the brake sub pump to perform axial transmission in the braking process, which not only changed the braking pressure but also led to an uneven distribution of the contact pressure [41], thereby causing jitter and high braking noise. In addition, the smaller the fluctuation in the friction coefficient of the specimen is, the less the possibility of self-excited vibration is, and the lower the probability of noise is [42]. The friction efficient fluctuation of Specimen Z3 with 4 wt.% zinc powder was the lowest, except under low-speed braking (40 km/h), regardless of whether it was subjected to high-speed braking or high-temperature fade (Fig. 6). This changing trend was consistent with that of the noise occurrence probability, which could further explain the influence of the zinc powder content on the braking noise of brake friction materials. Therefore, the addition of 4 wt.% zinc powder to friction brake material not only stabilized the friction coefficient, but also reduced the braking noise of the brake friction materials.

5 Conclusions

(1) With increasing zinc content, the density and thermal conductivity of the brake friction material increase but the hardness decreases. The addition of zinc powder shows no significant influence on the compression deformation behavior, shear strength, porosity or pH value of the brake friction materials.

(2) The nominal friction coefficient first increases, then decreases and finally increases again, while the lowest friction coefficient always gradually increases with increasing zinc content. The addition of 4 wt.% zinc powder into the friction materials is conducive to improving the stability of the high-temperature friction coefficient. The brake material with 4 wt.% zinc powder shows the best wear resistance.

(3) An appropriate addition of zinc powder is beneficial to inhibiting the generation of braking noise in the friction materials. The probability of noise occurrence first decreases and then increases with an increase of the zinc powder content. The brake friction material with 4 wt.% zinc powder shows excellent noise resistant performance.

References

[1] YUN R P, FILIP P, LA Y F. Performance and evaluation of eco-friendly brake friction materials [J]. Tribology International, 2010, 43: 2010−2019.

[2] STRAFFELINI G, MAINES L. The relationship between wear of semimetallic friction materials and pearlitic cast iron in dry sliding [J]. Wear, 2013, 307: 75−80.

[3] NOSKO O, BORRAJO-PELAEZ R, HEDSTRÖM P, OLOFSSON U. Porosity and shape of airborne wear microparticles generated by sliding contact between a low-metallic friction material and a cast iron [J]. Journal of Aerosol Science, 2017, 113: 130−140.

[4] RAJKUMAR G, SRINIVASAN J, SUVITHA L. Natural protein fiber hybrid composites: Effects of fiber content and fiber orientation on mechanical, thermal conductivity and water absorption properties [J]. Journal of Industrial Textiles, 2013, 44: 709−724.

[5] LEONARDI M, MENAPACE C, MATĚJKA V, GIALANELLA S, STRAFFELINI G. Pin-on-disc investigation on copper-free friction materials dry sliding against cast iron [J]. Tribology International, 2018, 119: 73−81.

[6] QU Xiong-wei, ZHANG Liu-cheng, DING Hui-li, LIU Guo-dong. The effect of steel fiber orientation on frictional properties of asbestos-free friction materials [J]. Polymer Composites, 2004, 25: 94−101.

[7] BIJWE J, KUMAR M. Optimization of steel wool contents in non-asbestos organic (NAO) friction composites for best combination of thermal conductivity and tribo-performance [J]. Wear, 2007, 263: 1243−1248.

[8] HO S C, CHERN LIN J H, JU C P. Effect of fiber addition on mechanical and tribological properties of a copper/ phenolic-based friction material [J]. Wear, 2005, 258: 861−869.

[9] NOH H J, JANG H. Friction instability induced by iron and

iron oxides on friction material surface [J]. Wear, 2018, 400−401: 93−99.

[10] KUMAR M, BIJWE J. Optimized selection of metallic fillers for best combination of performance properties of friction materials: A comprehensive study [J]. Wear, 2013, 303: 569−583.

[11] PARK S B, CHO K H, JUNG S, JANG H. Tribological properties of brake friction materials with steel fibers [J]. Metals and Materials International, 2009, 15: 27−32.

[12] KUMAR M, BIJWE J. Composite friction materials based on metallic fillers: Sensitivity of μ to operating variables [J]. Tribology International, 2011, 44: 106−113.

[13] TALIB R J, NOOR I I, MOHD F I, ABU OTHMAN E. Influence of steel fibres on friction behaviors with respect to speed, pressure and temperature [J]. Industrial Lubrication & Tribology, 2017, 69(3): 420−424.

[14] BAKLOUTI M, CRISTOL A L, DESPLANQUES Y, ELLEUCH R. Impact of the glass fibers addition on tribological behavior and braking performances of organic matrix composites for brake lining [J]. Wear, 2015, 330−331: 507−514.

[15] STOICA N A, PETRESCU A M, TUDOR A, PREDESCU A. Tribological properties of the disc brake friction couple materials in the range of small and very small speeds [J]. IOP Conference Series: Materials Science and Engineering, 2017, 174(1): 012019.

[16] YANG Ye-feng, JIN Yi-zheng, HE Hai-ping, WANG Qing-ling, TU Yao, LU Huan-ming, YE Zhi-zhen. Dopant-induced shape evolution of colloidal nanocrystals: The case of zinc oxide [J]. Journal of the American Chemical Society, 2010, 132: 13381−13394.

[17] KALYANI, RASTOGI R B, KUMAR D. Synthesis, characterization, and tribological evaluation of SDS-stabilized magnesium-doped zinc oxide ($Zn_{0.88}Mg_{0.12}O$) nanoparticles as efficient antiwear lubricant additives [J]. ACS Sustainable Chemistry & Engineering, 2016, 4: 3420−3428.

[18] ZHANG Ran-ran, LIU Xu-jie, XIONG Zhi-yuan, HUANG Qian-li, YANG Xing, YAN Hao, MA Jing, FENG Qing-ling, SHEN Zhi-jian. The immunomodulatory effects of Zn-incorporated micro/nanostructured coating in inducing osteogenesis [J]. Artificial Cells, Nanomedicine, and Biotechnology, 2018, 46: 1−8.

[19] YU Yi-qiang, JIN Guo-dong, XUE Yang, WANG Dong-hui, LIU Xuan-yong, SUN Jiao. Multifunctions of dual Zn/Mg ion co-implanted titanium on osteogenesis, angiogenesis and bacteria inhibition for dental implants [J]. Acta Biomater, 2017, 49: 590−603.

[20] MAO Lin, ZHOU Hao, CHEN Li, NIU Jia-lin, ZHANG Lei, YUAN Guang-yin, SONG Cheng-li. Enhanced biocompatibility and long-term durability in vivo of Mg−Nd−Zn−Zr alloy for vascular stent application [J]. Journal of Alloys and Compounds, 2017, 720: 245−253.

[21] VERMA D K, KUMAR B, KAVITA, RASTOGI R B. Zinc oxide and magnesium doped zinc oxide decorated nanocomposites of reduced graphene oxide as friction and wear modifiers [J]. ACS Applied Materials & Interfaces, 2019, 11: 2418−2430.

[22] ÖSTERLE W, URBAN I. Friction layers and friction films on PMC brake pads [J]. Wear, 2004, 257: 215−226.

[23] SHIBATA K, GOTO A, YOSHIDA S, AZUMA Y, NAKAMURA K. Development of brake friction material [M]. Detroit: SAE International, 1993.

[24] ZHOU Wei. Application of SAE J2521 in the noise analysis of light-duty car disc brake [J]. Equipment Manufacturing Technology, 2013, 11: 193−194, 213. (in Chinese)

[25] ARANGANATHAN N, BIJWE J. Special grade of graphite in NAO friction materials for possible replacement of copper [J]. Wear, 2015, 330−331: 515−523.

[26] KUMAR M, BIJWE J. Studies on reduced scale tribometer to investigate the effects of metal additives on friction coefficient—Temperature sensitivity in brake materials [J]. Wear, 2010, 269: 838−846.

[27] JACKO M G, TSANG P H S, RHEE S K. Wear debris compaction and friction film formation of polymer composites [J]. Wear, 1989, 133: 23−28.

[28] ZHAO Na-na, ZHAO Yu-rong, WEI Yi-qi, WANG Xin, LI Jie, XU Yun-hua, YAN Fu-xue, LU Zheng-xin. Friction and wear behavior of TaC ceramic layer formed in-situ on the gray cast iron [J]. Tribology International, 2019, 135: 181−188.

[29] LAWN B R, EVANS A G, MARSHALL D B. Elastic/plastic indentation damage in ceramics: The median/radial crack system [J]. Journal of the American Ceramic Society, 1980, 63: 574−581.

[30] MAO Cong, LIANG Chang, ZHANG Yun-chen, ZHANG Ming-jun, HU Yong-le, BI Zhu-ming. Grinding characteristics of cBN−WC−10Co composites [J]. Ceramics International, 2017, 43: 16539−16547.

[31] CAI Peng, WANG Yan-ming, WANG Ting-mei, WANG Qi-hua. Effect of resins on thermal, mechanical and tribological properties of friction materials [J]. Tribology International, 2015, 87: 1−10.

[32] GAO Pei-hu, CHEN Bai-yang, WANG Wei, JIA Han, LI Jian-ping, YANG Zhong, GAO Yong-chun. Simultaneous increase of friction coefficient and wear resistance through HVOF sprayed WC−(nano WC−Co) [J]. Surface and Coatings Technology, 2019, 363: 379−389.

[33] CHUNG J, GO S, KIM J, KIM H, CHOI H. Conditions for transfer film formation and its effect on friction coefficients in NAO friction materials containing various abrasive components [J]. International Journal of Precision Engineering and Manufacturing, 2018, 19: 1011−1017.

[34] MAO Cong, ZHANG Yun-chen, PENG Xiao-xiao, ZHANG Bi, HU Yong-le, BI Zhu-ming. Wear mechanism of single cBN−WC−10Co fiber cutter in machining of Ti−6Al−4V alloy [J]. Journal of Materials Processing Technology, 2018, 259: 45−57.

[35] BAI L C, SRIKANTH N, KORZNIKOVA E A, BAIMOVA J A, DMITRIEV S V, ZHOU K. Wear and friction between smooth or rough diamond-like carbon films and diamond tips [J]. Wear, 2017, 372−373: 12−20.

[36] BAI L C, SRIKANTH N, KANG G Z, ZHOU K. Influence of third particle on the tribological behaviors of diamond-like carbon films [J]. Scientific Reports, 2016, 6(1): 38279.

[37] ZHAI Wen-zheng, ZHOU Kun. Nanomaterials in superlubricity [J]. Advanced Functional Materials, 2019,

29(28): 1806395.

[38] FEDERICI M, ALEMANI M, MENAPACE C, GIALANELLA S, PERRICONE G, STRAFFELINI G. A critical comparison of dynamometer data with pin-on-disc data for the same two friction material pairs—A case study [J]. Wear, 2019, 424−425: 40−47.

[39] KCHAOU M, MAT LAZIM A R, ABU BAKAR A R, FAJOUI J, ELLEUCH R, JACQUEMIN F. Effects of steel fibers and surface roughness on squealing behavior of friction materials [J]. Transactions of the Indian Institute of Metals, 2016, 69: 1277−1287.

[40] WANG D W, MO J L, GE X H, OUYANG H, ZHOU Z R. Disc surface modifications for enhanced performance against friction noise [J]. Applied Surface Science, 2016, 382: 101−110.

[41] BRYANT D, FIELDHOUSE J D, TALBOT C J. Brake judder—An investigation of the thermo-elastic and thermo-plastic effects during braking [J]. International Journal of Vehicle Structures and Systems, 2011, 3: 58−73.

[42] YANG S, GIBSON R F. Brake vibration and noise: Reviews, comments, and proposals [J]. International Journal of Materials and Product Technology, 1997, 12: 496−513.

锌粉含量对汽车制动摩擦材料摩擦学性能的影响

杨 阳[1,2*]，梁陆新[1*]，吴 宏[1]，刘伯威[1,2]，瞿 辉[2]，方琪洪[3]

1. 中南大学 粉末冶金国家重点实验室，长沙 410083；
2. 湖南博云汽车制动材料有限公司，长沙 410205；
3. 湖南大学 车身先进设计与制造国家重点实验室，长沙 410082

摘 要：采用粉末冶金法制备具有不同锌粉含量(0，2%，4%，6%，8%，质量分数)的汽车制动摩擦材料。结果表明，随着锌粉含量的增加，材料的密度和导热系数逐渐增加，而硬度呈单调下降趋势。随着锌粉含量的增加，标称摩擦因数曲线呈波动趋势，但最低摩擦因数呈现增加趋势。然而，随着锌含量的增加，摩擦材料的磨损率和制动噪声单调递减，这是因为摩擦机理从粘着磨损和磨粒磨损转变为粘着磨损。含 4% (质量分数)锌粉的制动摩擦材料表现出最佳的摩擦学和抗噪声性能.

关键词：锌粉含量；刹车摩擦材料；摩擦行为；刹车噪音

(Edited by Wei-ping CHEN)